Consideration of Two-Dimensional Flow Effects on Nozzleless Rocket Performance

Merrill K. King*
Atlantic Research Corporation, Alexandria, Virginia

Abstract

A NUMERICAL analysis procedure has been developed for examination of two-dimensional flow effects on nozzleless rocket motor performance. In this analysis, it is assumed that there are no radial variations in static pressure and that flow is isentropic along each streamtube. Performance predictions are compared with standard one-dimensional flow predictions. It is found that two-dimensional effects on performance are considerably less than predicted by previous analyses, with a maximum increase in vacuum throat specific impulse of only 2.0%. As expansion ratio considerations are brought in, the performance difference decreases to less than 1%.

Contents

Theoretical performance calculations for solid rocket motors (including nozzleless motors) are generally performed with assumption of one-dimensional flow. However, it has been observed[1-3] that for low L/D motors and/or high blowing rates, the flow in typical cylindrically perforated motors (particularly nozzleless motors) is highly two-dimensional. Thus, mass is injected from the grain into a zero or very low-velocity flow region all along the port instead of being injected directly into a high-velocity crossflow in the downstream regions (as in the one-dimensional idealization). This can result in a considerably less irreversible flow situation, with resultant increase in the availability function (potential for conversion of thermal to kinetic energy) for the actual two-dimensional flow. Previous analyses of this situation by Glick[4,5] are reviewed by King[6]. In his first paper, Glick concluded that vacuum throat specific impulse values 10% higher than one-dimensional values would result from two-dimensional flow considerations, while in his second paper he concluded that the difference was 4 to 5%.

In the current study, streamtube tracking has been employed to calculate the flow profile development (and accompanying wall pressure distribution) from the head-end of a straight-bore nozzleless motor to the choke point (defined by approach to a singularity in the equation set associated with attainment of a maximum allowable mass flow for the given cross-sectional area and head-end pressure). In this analysis, it has been assumed that radial static pressure gradients can be neglected and that flow along each streamtube is isentropic (inviscid flow assumption). An outline of the analysis follows; more details appear in Ref. 6. Comparative one-dimensional calculations were performed using the influence coefficient approach outlined by Shapiro.[7]

First, the grain port radius and head-end pressure are specified along with flame temperature, product molecular weight, specific heat ratio and a relationship between mass burning flux and pressure (Vielle's Law). A small axial increment is chosen and the static pressure (assumed independent of radial location) at the end of the increment is guessed. The increment is then divided into N subincrements, each defining the axial location of the starting point of a steamtube. It is assumed that pressure varies linearly along the increment (sufficiently accurate for suitably small increments) thus permitting calculation of total pressure associated with each streamtube. (Since reversible flow is assumed for each streamtube, total pressure is constant along any given tube and is essentially equal to wall pressure at the origin of that tube). From the burning rate versus pressure relationship and given flame temperature and product molecular weight, velocity into each streamtube and total mass flow rate through each tube are straightforwardly calculated. At this point, static and total pressure are known for each streamtube at the end of the increment being analyzed, permitting calculation of velocity, density, area, etc. of each streamtube at this axial location. (Geometric arguments are used to specify angular orientation of the streamtubes and thus projected areas perpendicular to the port axis.) Mass continuity is then used to calculate the inner radius of each streamtube (starting from the wall) at the end of the increment. If the inner radius of the innermost tube does not come out sufficiently close to zero, a new value of static pressure at the end of the increment is guessed, with looping to convergence.

Next, another axial increment is chosen and another N streamtubes added to the analysis—this procedure is repeated (with increment sizes being adjusted as needed to keep pressure drop over any increment small) until the procedure fails in the vicinity of the singular choke point, thus defining the grain length consistent with the assigned head-end pressure (an inverse solution procedure). A rather careful end-game procedure permits definition of this location (and thus vacuum throat specific impulse) to within 0.01%. Subsequent area expansion (made possible through provision of a chamfered surface at the end of the grain) is then treated straightforwardly (again assuming negligible radial static pressure gradients and isentropic flow along each streamtube) for calculation of stream thrust and area of each streamtube at any desired expansion pressure. The vacuum throat specific impulse is calculated as the product of head-end pressure and port area divided by total flow rate, while specific impulse vs expansion ratio for any given ambient pressure is calculated via:

$$\epsilon = \Sigma A_j^*(A/A^*)_j / A_{\text{port}} \tag{1}$$

$$I_{sp} = [\sqrt{2(\gamma+1)RT_{\text{flame}}/g\gamma(MW)}\,\Sigma(F/F^*)_j W_{\text{TOT},j} - P_{\text{amb}} R_{\text{port}} \epsilon] / \Sigma_{\text{TOT},j} \tag{2}$$

where the summations are performed over the j streamtubes (N times number of increments analyzed).

A series of parametric calculations were performed using the analysis outlined above. In each case, specification of head-end pressure (for a given port radius) resulted in a unique motor length. This same length motor was then analyzed on a one-dimensional basis (resulting in slightly lower head-end pressure), since it was judged to be more appropriate to hold motor dimensions constant than to hold head-end pressure

Presented as Paper 84-1313 at the AIAA/SAE/ASME 20th Joint Propulsion Conference, Cincinnati, OH, June 11-13, 1984; received July 5, 1984; synoptic received June 4, 1986.

*Manager, Combustion Research Department, Research and Technology Division. Associate Fellow AIAA.

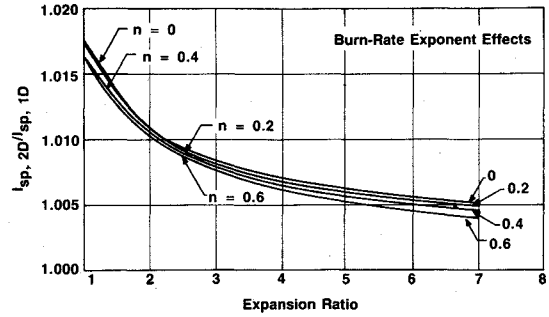

Fig. 1 Burn-rate exponent effects on two-dimensional I_{sp}/one-dimensional I_{sp} ratio vs expansion ratio.

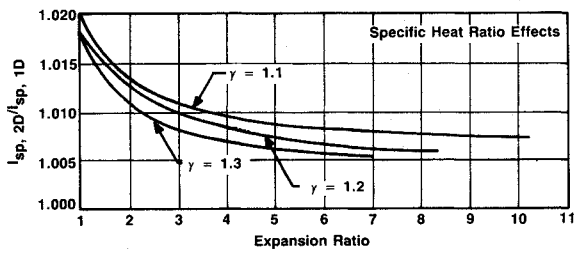

Fig. 2 Specific heat ratio effects on two-dimensional I_{sp}/one-dimensional I_{sp} ratio vs expansion ratio.

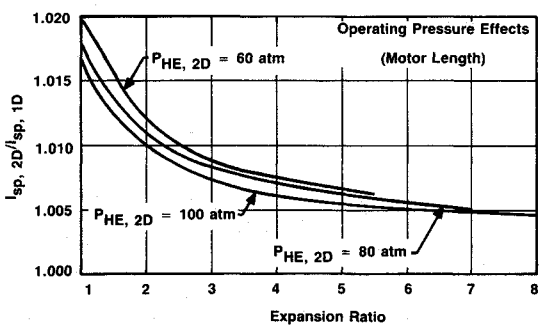

Fig. 3 Operating pressure effects on two-dimensional I_{sp}/one-dimensional I_{sp} ratio vs expansion ratio.

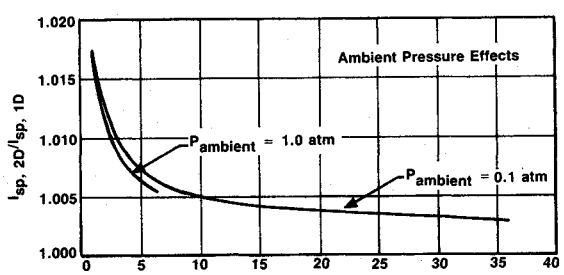

Fig. 4 Ambient pressure effects on two-dimensional I_{sp}/one-dimensional I_{sp} ratio vs expansion ratio.

constant in comparison of one- and two-dimensional performance predictions.

As a baseline case, burning mass flux was fixed at 3.0 gm/cm^{2}s, independent of pressure (burn-rate exponent = 0), specific heat ratio was 1.3, flame temperature was 3000 K, product molecular weight was 30, port radius was 1.5 cm, and grain length was 116.24 cm. With the two-dimensional analysis, resulting head-end pressure was 80.0 atm, vacuum throat specific impulse was 177.92 s, and throat pressure was 31.0 atm ($P_{throat}/P_{head\ end} = 0.386$) while for the comparable one-dimensional analysis, the head-end pressure was calculated to be 78.64 atm, vacuum throat specific impulse was 174.85 s, and throat pressure was 34.19 atm ($P_{throat}/P_{head\ end} = 0.435$). Thus it may be seen that for the baseline case the increase in vacuum throat specific impulse associated with flow two-dimensionality is only 1.74%, and that it is accompanied by a decrease in throat-to-head-end pressure ratio from 0.435-0.386, with a consequent decrease in availability for thermal-kinetic energy conversion during expansion. Comparison of the axial velocity profile at the throat predicted with this analysis with an incompressible flow inviscid no-wall-slip cosine profile (used in Ref. 4) shows that the actual profile is considerably more "filled" than the cosine profile, resulting in less nonlinear averaging effects in determination of the vacuum throat specific impulse: this explains the decrease from 10% higher values for this parameter relative to one-dimensional values (as calculated in Ref. 4) to the 1.74% difference between two- and one-dimensional values calculated with this more detailed analysis. In addition, the ratio of specific impulse calculated using two-dimensional analysis to that calculated using one-dimensional analysis decreases with increasing expansion area ratio due to the reduced availability for thermal-kinetic energy conversion. For example, for matched expansion to one atmosphere ambient pressure, the specific impulse calculated for this baseline case with the two-dimensional analysis is only 0.50% higher than the one-dimensional values.

Effects of burn-rate exponent, specific heat ratio, operating pressure (determined by grain length and port radius), and ambient pressure on ratio of two-dimensional specific impulse to one-dimensional specific impulse vs expansion ratio are delineated in Figs. 1-4. As may be seen from Fig. 1, burn-rate exponent effects are rather small, with a slight decrease in specific impulse ratio accompanying an increase in exponent from 0.0-0.6. Specific heat ratio effects (Fig. 2) are somewhat larger, with the specific impulse ratio increasing with decreasing specific heat ratio. Increasing operating pressure leads to a decrease of the two-dimensional flow effects on performance (Fig. 3), while decreasing ambient pressure for a given expansion ratio results in slightly larger effects (Fig. 4) though the matched expansion two-dimensional/one-dimensional specific impulse ratio decreases from 1.005-1.002 as ambient pressure decreases from 1.0-0.1 atm. Thus, it appears that two-dimensional flow effects have, at most, a second-order influence on nozzleless motor performance, contrary to results obtained by Glick.[4,5]

References

[1]Culick, F.E.C., "Rotational Axisymmetric Mean Flow and Damping of Acoustic Waves in a Solid Propellant Rocket," *AIAA Journal,* Vol. 4, Aug. 1966, p. 1462.

[2]Dunlap, R., Willoughby, P.G., and Hermsen, R.W., "Flowfield in the Combustion Chamber of a Solid Propellant Rocket Motor," *AIAA Journal,* Vol. 12, Oct. 1974, pp. 1440-1442.

[3]Yamada, K., Goto, M., and Ishikawa, N., "Simulative Study on the Erosive Burning of Solid Rocket Motors," *AIAA Journal,* Vol. 14, Sept. 1976, pp. 1170-1776.

[4]Glick, R.L. and Orr, C.E., "On the Idealized Performance of Nozzleless Rocket Motors," AIAA Paper 80-1137, 1980.

[5]Glick, R.L., "On the Performance of Nozzleless Rocket Motors," AIAA Paper 83-1318, 1983.

[6]King, M.K., "Consideration of Two-Dimensional Flow Effects on Nozzleless Rocket Performance," AIAA Paper 84-1313, 1984.

[7]Shapiro, A.H., *The Dynamics and Thermodynamics of Compressible Fluid Flow,* Vol. I, The Ronald Press Co., New York, 1953, p. 228.